Biochimica et Biophysica Acta 1840 (2014) 3357–3366

Contents lists available at ScienceDirect

Biochimica et Biophysica Acta

journal homepage: www.elsevier.com/locate/bbagen

Interactions of cellular histidine triad nucleotide binding protein 1 with nucleosides 5′-*O*-monophosphorothioate and their derivatives — Implication for desulfuration process in the cell

Agnieszka Krakowiak *, Róża Pawłowska, Beata Kocoń-Rębowska, Rafał Dolot, Wojciech J. Stec

Centre of Molecular and Macromolecular Studies, Polish Academy of Sciences, Department of Bioorganic Chemistry, Lodz, Poland

ARTICLE INFO

Article history:
Received 30 April 2014
Received in revised form 20 August 2014
Accepted 28 August 2014
Available online 6 September 2014

Keywords:
Hint1
Photocrosslink
siRNA
(d)NMPS
PS-oligo metabolism
Hydrogen sulfide

ABSTRACT

Background: One of the activities of histidine triad nucleotide-binding protein 1 (Hint1) under *in vitro* conditions is the conversion of nucleoside 5′-*O*-phosphorothioate (NMPS) to its 5′-*O*-phosphate (NMP), which is accompanied by the release of hydrogen sulfide.
Methods: Non-hydrolyzable derivatives of AMPS and dCMPS, each containing the residue able to form a covalent bond in nucleic acid–protein complexes *via* photocrosslinking (at 308 nm), were applied at the complexing experiments with recombinant and cellular Hint1.
The cellular lysates prepared after RNAi-mediated knockdown of Hint1 were incubated with AMPS and the level of desulfuration was measured.
Results: Recombinant Hint1 and Hint1 present in the cellular lysate of A549 cells, formed complexes with the used substrate analogs.
Computer modeling experiments, in which the ligand was docked at the binding pocket, confirmed that direct interactions between Hint1 and the screened analogs are possible.
Using RNAi technology, we demonstrated lowered levels of AMPS substrate desulfuration in reactions that employed the cell lysates with a reduced Hint1 level.
Conclusions: The enzymatic conversion of AMPS to AMP occurred with the participation of cellular Hint1, the protein, which is present in all organisms.
General significance: The intracellular Hint1 could be responsible for the *in vivo* desulfuration of nucleosides-5′-monophosphorothioate, thus it can contribute to the phosphorothioate oligonucleotides metabolism. H_2S released during this process may participate in several physiological processes, thus NMPSs can be precursors/donors of H_2S *in vivo* and can be used to study the effects of this gas in biological systems. Moreover, the controlled delivery of (d)NMPSs into cells may be of medicinal utility.

1. Introduction

Histidine triad nucleotide binding protein 1 (Hint1) is a cytosolic enzyme (126 amino acids) belonging to the most ancient branch of the histidine triad protein superfamily (HIT) [1]. These proteins exert their activities as hydrolases or transferases, and they are characterized by an H–X–H–X–H–X–X–X sequence motif (H is a histidine residue, and X is a hydrophobic amino acid) at their catalytic center. Hint1 is ubiquitously expressed in both prokaryotes and eukaryotes. Prokaryote genomes, including those of bacteria, typically encode one HINT gene, but eukaryotes generally express multiple HINT forms. The HIT motif has been highly conserved throughout evolution, but the correlation between the cellular function and enzymatic activity of these proteins is not particularly clear.

In vitro, Hint1 accepts many substrates containing phosphate linkages of different types, such as phosphoramidates (AMP-NH_2 and AMP-*N*-ε-lysine [2], the cleavage of the P–N bond), acyl-phosphates (lysyl-AMP, the cleavage of the P–O bond [3]), phosphorothioates of ribo- and 2′-deoxyribonucleoside series ((d)NMPS [4], the cleavage of the P–S bond) and phosphorofluoridates (adenosine-5′-*O*-phosphorofluoridate [5], the cleavage of the P–F bond). Thus, Hint1 catalyzes the degradation of compounds that contain the general formula NMP–X (X = NHR, OC(O)R, S or F), and hydrolysis yields NMP and an X-residue (Fig. 1). Substrate specificity studies have revealed a Hint1 preference for nucleoside phosphoramidates (NMP-NHR) and phosphorothioates (NMPS) containing purines over pyrimidines and ribose over 2′-deoxyribose [4,6], and nucleoside acyl-monophosphates (NMP-OC(O)R) were found to

Abbreviations: Hint1, histidine triad nucleotide-binding protein 1; PS-oligos, oligo(nucleoside phosphorothioate)s; AMPS, adenosine 5′-*O*-monophosphorothioate; (d)NMPS, (deoxy)nucleoside 5′-*O*-monophosphorothioate

* Corresponding author at: Centre of Molecular and Macromolecular Studies, Polish Academy of Sciences, Department of Bioorganic Chemistry, Sienkiewicza 112, 90-363 Lodz, Poland. Tel.: +48 42 6803272; fax: +48 42 6815483.
E-mail address: akrakow@cbmm.lodz.pl (A. Krakowiak).

http://dx.doi.org/10.1016/j.bbagen.2014.08.016
0304-4165/

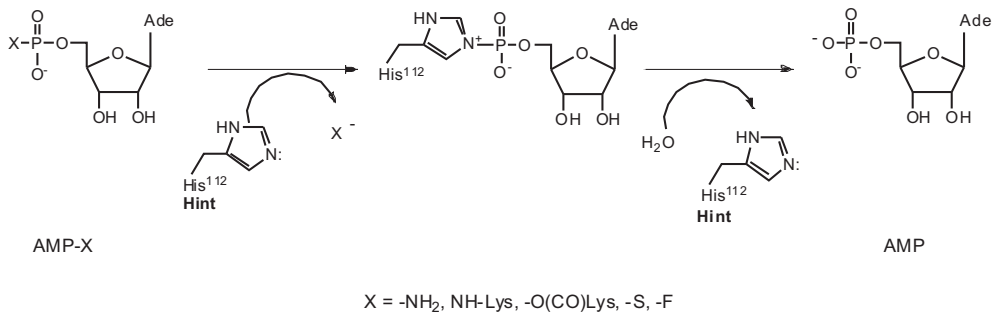

Fig. 1. The reaction scheme for Hint1 catalysis of the hydrolysis of NMP-X substrates [1,4].

be slightly better substrates than NMP-NHR [3] and much better substrates than NMPS [4].

Little is known about the possible connection between the enzymatic activity and intracellular function(s) of Hint1. To date, the majority of its known functionalities appear to be unrelated to its enzymatic mode of action. Hint1 acts as a tumor suppressor *via* a mechanism that relies on the induction of apoptosis [7]. Following transient transfection with Hint1, cells undergo apoptosis through the mitochondrial pathway, which includes cytochrome *c* release and caspase-3 activation. However, the H112N mutant (which is unable to hydrolyze AMP-NH_2) still induces apoptosis; thus, Hint1 pro-apoptotic activity is independent of Hint1 enzymatic activity. Additionally, Hint1 interacts with pontin and reptin, inhibiting the β-catenin pathway of Wnt target gene transcription, and this function is also independent of its enzymatic activity [8]. Another intracellular role of Hint1 that is not connected to its hydrolytic activity is the regulation of the Mu opioid receptor in the nervous system. This regulation is exerted by the formation of complexes with certain signaling proteins (*e.g.*, the Mu-opioid receptor (MOR), the glutamate N-methyl-D-aspartate receptor (NMDAR), protein kinase C (PKC), the serine/threonine kinase Raf-1 and a regulator of G protein signaling Z2 (RGSZ2) [9]).

Eukaryotic Hint1 is associated with gene transcription factors such as TFIIH [10], microphthalmia transcription factor (MITF) [11,12] and upstream stimulatory factor 2 (USF2) [13]. Hint1 enzymatic activity is necessary for yeast to grow on galactose at elevated temperatures, which is connected to the inhibition of Kin28 (a part of TFIIH), most likely through the accumulation of a Hint/Hnt1 substrate (Hnt1 is the Hint1 analog in yeast) [2]. Similar interactions have been suggested for Cdk7, the human equivalent of Kin28. A functional multiprotein interaction between Hint1, lysyl-tRNA synthetase (LysRS) and MITF [12], in addition to USF2 [13], has been documented. Both of these transcription factors can affect tumorigenesis signaling pathways and are inhibited when associated with Hint1. After the activation of LysRS by phosphorylation, the production of the signaling molecule diadenosine tetraphosphate (Ap_4A) occurs from the condensation of Lys-AMP, the intermediate product of LysRS. Ap_4A then binds Hint1 and induces Hint1 dissociation from MITF or USF2, which allow for the trans-activation of transcription factors [14]. In the above mechanism of transcriptional regulation, Hint1 can bind and hydrolyze Lys-AMP [15], and this destruction reaction could constrain Ap_4A production. Thus, the hydrolytic activity of Hint1 may extend beyond Lys-AMP and could be connected to the control of Ap_4A level.

Hint1 enzymatic activity (ecHinT) is necessary for *Escherichia coli* growth under high-salt conditions [16] and for growth on alanine, which is connected to the activity of *E. coli* D-alanine dehydrogenase [17]. Recently, the relationship of the first phenotype to hHint1 (human Hint1) enzymatic activity has been identified. Inherited peripheral neuropathy is caused by the loss of the enzymatic function of this protein [18]. A strong connection between the loss of catalytically functional hHint1 and autosomally recessive axonal neuropathy with neuromyotonia has been demonstrated by genome SNP analysis.

Our *in vitro* studies of the desulfuration of adenosine 5′-*O*-phosphorothioate by Hint1 indicated a relationship between enzymatic activity and cellular function. Cleavage of the P – S bond with AMP and H_2S release [4] may be biologically significant because hydrogen sulfide is a cellular gaseous mediator that participates in multiple physiological processes, *e.g.*, blood pressure regulation [19], protection against stress and pain sensing and participation in learning and memorization processes [20]. Inside organisms, H_2S is enzymatically produced by amino acid metabolism and can cause posttranslational modification of proteins. Molecular targets for H_2S include ATP-sensitive K^+ channels connecting H_2S with the modulation of the vascular tone *in vivo* [21]. On the other hand, besides AMPS, other 5′-*O*-phosphorothioylated ribonucleosides (GMPS, CMPS, and UMPS) and corresponding 5′-*O*-phosphorothioylated deoxyribonucleosides are also desulfurated by Hint1, and the rates of sulfur loss vary from ~0.2 nmol min^{-1} μg^{-1} for AMPS to 0.00057 nmol min^{-1} μg^{-1} for TMPS [4]. Therefore, we cannot exclude the possibility that Hint1 participates in the metabolism of 5′-*O*-phosphorothioate derivatives of ribonucleosides or 2′-deoxyribonucleosides under cellular conditions. A few years ago, this observation would have had limited importance because nucleoside 5′-*O*-monophosphorothioates were believed to appear in cells only as a result of the enzymatic degradation of the phosphorothioate or phosphoramidothioate analogs of oligonucleotides or nucleotides. However, in 2007 phosphorothioate DNA segments were identified in bacterial DNA [22], and it became clear that the biology of phosphorothioate nucleotides requires much deeper consideration. The enzymes responsible for the *in vivo* degradation of PS-oligonucleotides (which were developed as antisense probes for genomic research and for medicinal applications as anticancer or antiviral drugs [23]) are well known (*e.g.*, 3′-exonuclease from plasma) [24,25]; however, the metabolism of (d)NMPS has not been explored in-depth. These relatively small molecules may modulate many processes, *e.g.*, the proliferation of cells (stimulation, inhibition and cytotoxicity), as well as DNA and RNA synthesis [26,27].

Here, we present the results of our recent study on the possible desulfuration of NMPS by the Hint1 protein in the cellular milieu. Using the photocrosslinking method [28], we found that recombinant Hint1 forms complexes with certain non-hydrolyzable analogs of (d)NMPS. Similar complexes were observed for Hint1 protein present in cellular extracts that were obtained from A549 cells. These cells were free of Fhit ($Fhit^-$), which is another member of the HIT family [1]. Additionally, AMPS desulfuration level was measured using cell lysates (A549 and Hela cells, both $Hint1^+$ and $Fhit^-$). We observed a decrease in the loss of sulfur from AMPS when using lysates from cells in which Hint1 was silenced (*via* siRNA targeted to HINT1 mRNA) compared to reactions with control lysates from cells that were transfected with non-specific siRNA. These results suggest that intracellular Hint1 can be responsible for the desulfuration of adenosine-5′-*O*-phosphorothioate in the cell.

2. Materials and methods

2.1. Synthesis, purification and labeling of *PS-A* and *PS-dC*

The solid-phase synthesis of compounds **PS-A** and **PS-dC** was performed on a 0.5 μmol scale by a standard phosphoramidite procedure

with sulfurization. Empty columns were packed with *N*-Pac-A-CPG (5′-*O*-dimethoxytrityl-2′-*O*-acetyl-*N*-phenoxyacetyl-adenosine-3′-*O*-succinoyl-long chain alkylamino-CPG) or *N*-Bz-dC-CPG (5′-*O*-dimethoxytrityl-*N*-benzoyl-2′-deoxycytidine-3′-*O*-succinoyl-long chain alkylamino-CPG) (both supplied by Glen Research, USA). After deprotection of the 5′-OH group with 3% dichloroacetic acid (DCA) in CH_2Cl_2, 10 μmol of 3-(4,4′-dimethoxytrityloxy)propyl-1-(2-cyanoethyl)-*N*,*N*-diisopropyl phosphoramidite (Glen Research, USA) and a 1 M solution of 5-(ethylthio)-tetrazole in anhydrous CH_3CN were added to the reaction column. After 10 min of coupling, a 1 M solution of bis(*O*,*O*-diisopropoxy phosphinothioyl) disulfide (S-*tetra*, a sulfurizing reagent [29]) in CH_3CN/pyridine was applied for 10 min, followed by the removal of the DMT group and another coupling reaction, this time with 10 μmol of 5Br-dU phosphoramidite (5′-*O*-dimethoxytrityl-5-bromo-2′-deoxyuridine-3′-*O*-(2-cyanoethyl-*N*,*N*-diisopropyl phosphoramidite)) or 4-thio-dU phosphoramidite (5′-*O*-dimethoxytrityl-2′-deoxy-4-(2-cyanoethylthio)-uridine-3′-*O*-(2-cyanoethyl-*N*,*N*-diisopropyl phosphoramidite)) in the presence of 5-(ethylothio)-tetrazole in CH_3CN. Then, the bound to the support P^{III} intermediate product was sulfurized with an S-*tetra* solution in CH_3CN/pyridine. The resulting compound containing a 5Br-dU residue was cleaved from the solid support with 28% NH_4OH (4 h at room temperature), and the cleavage was accompanied by the removal of the acetyl, phenoxyacetyl and 2-cyanoethyl protecting groups. The compound containing the 4S-dU residue was deprotected with 50 mM NaSH in NH_4OH for 24 h at room temperature to maintain the sulfur atom at the 4 position of the nucleobase. Both compounds were isolated by two-step (DMT-ON, DMT-OFF) reversed-phase HPLC purification with a BDS-Hypersil 300 × 4.6 mm column (Thermo Scientific), a flow rate of 1.0 ml/min, and with the following mobile phase: a 0–40% CH_3CN gradient in 0.1 M triethylammonium bicarbonate (TEAB, pH 7.4).

After the DMT-ON step (CH_3CN gradient 0.75%/min), 3 fractions containing diastereomers of **PS-A** were collected at the retention times of 27.75 min (f1), 28.57 min (f2) and 28.89 min (f3). The molecular masses of the isolated products were confirmed by MALDI-TOF MS (m/z 1105.2, calc. 1106.1). A second purification step was performed (DMT-OFF) after removing the dimethoxytrityl group from each isolated fraction (using a 3% DCA solution in methylene chloride for 30 min). During the chromatography run, fraction 1 produced two peaks (1a and 1b), and therefore a total of four **PS-A** fractions (1a, 1b, 2 and 3) that contained four possible diastereoisomers (due to the chirality of two phosphorus atoms) were obtained. The molecular masses of the isolated products were confirmed by MALDI-TOF MS (m/z = 804.08, calc. = 803.1). The total amount of all four **PS-A** diastereomers was 3 OD units.

The analogous two-step **PS-dC** purification yielded two fractions of 0.7 OD (**PS-dC1**) and 0.9 OD (**PS-dC2**), and their molecular masses were determined by MALDI-TOF MS (m/z = 701.7, calc. = 702).

All compounds (1.2 nmol of each) were labeled at the 5′-end with T4 polynucleotide kinase (10 U) (Fermentas/Thermo Scientific) and 0.08 mCi [γ^{32}P]ATP (Hartmann Analytic, Germany) in a standard buffer (20 μl total volume). The reactions were performed for 20 h at 37 °C and were terminated by heating at 95 °C for 3 min.

The purity of the resulting compounds was checked by PAGE. The samples (1/20 of the reaction mixture + 3 μl of formamide containing 0.1% bromophenol blue) were loaded onto a 20% polyacrylamide gel under denaturing conditions (7 M urea and TBE buffer). The developed gels were autoradiographed and analyzed by GeneTools 4.00 software.

A **T-PO-A** dinucleotide, which did not contain a moiety for photocrosslinking at 312 nm, was synthesized in a manner similar to that of the **PS-A** dimer and instead of a sulfurization step (with S-*tetra*, a sulfurizing reagent), the P^{III} intermediate product was oxidized by a routine reagent I_2/H_2O/pyridine.

2.2. Purification of wild-type (wt) Hint1

Rabbit Hint1 protein was expressed from plasmid pSGA02 [30] in the *E. coli* strain BL 21*. Hint1 was purified according to a published procedure [2] using AMP-agarose (Sigma-Aldrich) affinity chromatography. Homogenous enzyme preparations were dialyzed against a buffer containing 20 mM Tris (pH 7.5) and 150 mM NaCl, and they were concentrated to 10 mg/ml and stored at −80 °C.

2.3. Cell lines

All cell lines, HeLa (human cervix carcinoma) and A549 (human lung carcinoma) were grown at 37 °C in a 5% CO_2 atmosphere with an additional 100 U/l of penicillin G and 100 U/l of streptomycin in RPMI 1640 medium (Sigma-Aldrich) supplemented with 10% fetal bovine serum (FBS) (Gibco/Life Technologies).

2.4. Extract preparation

Cells were trypsinized (using 2.5% trypsin in phosphate buffered saline (PBS)) and then washed twice with PBS. Next, the cells were suspended in a buffer containing 10 mM HEPES, 10 mM NaCl, 1 mM KH_2PO_4, 5 mM $NaHCO_3$, 1 mM $CaCl_2$, 0.5 mM $MgCl_2$, 5 mM EDTA and protease inhibitors (Complete®, Roche, Penzberg, Germany) (CLB/EDTA/PI). After 5 min of incubation on ice, the cells were sonicated (2 × 30 s) and centrifuged (7500 rpm, 5 min). Finally, the supernatants (the cytosolic fractions) were purified using Zeba Spin Desalting Columns (7 K MWCO, Thermo Scientific) to remove small nucleic acid molecules.

2.5. Western blot analysis

Proteins from the cytosolic fractions of the cell lysates (20 μg) for each sample were separated on a 4%/15% Tris–glycine SDS-PAGE gel and electroblotted to a PVDF membrane (Millipore). The filter was blocked in 5% non-fat dry milk, incubated with rabbit primary antibodies (against Hint1 (Proteintech), or GAPDH (Santa Cruz Biotechnology, Santa Cruz, CA, USA)), washed, probed with goat anti-rabbit IgG conjugated to alkaline-phosphatase (Zymed) and developed with Immobilon Western Chemiluminescence AP Substrate (Millipore). The signals were visualized by using a G-Box (SynGene, Cambridge, England) instrument with a chemiluminescent camera, and they were analyzed by GeneTools 4.00 software. Hint1 expression levels were calculated as the ratio of Hint1 signal intensity to GAPDH signal intensity.

2.6. Enzymatic reactions

The degradation of [^{32}P]-5′-end-labeled dimers in **PS-A** (0.12 nmol) with nuclease P1 (nP1, Sigma-Aldrich) or snake venom phosphodiesterase (*sv*PDE, Sigma-Aldrich) was performed in a 10-μl volume at 37 °C for 5 h and 24 h in a buffer containing 100 mM CH_3COONa (pH 7.0), 1 mM $ZnCl_2$ and 1 μg of nP1 or by the independent addition of 25 mM Tris HCl (pH 8.5), 5 mM $MgCl_2$ and 1 μg of svPDE.

Compounds **PS-A** and **PS-dC** were screened for hydrolysis catalyzed by the Hint1 enzyme in 10-μl reaction mixtures containing a [^{32}P]-5′-end-labeled substrate (0.12 nmol) and 6.0 μg of the enzyme in buffer H (20 mM HEPES-Na (pH 7.2) and 0.5 mM $MgCl_2$). The samples were incubated at 37 °C for 5 h or 20 h.

The reaction mixtures were quenched by cooling on ice and adding formamide (3 μl) containing 0.1% bromophenol blue, and then they were loaded onto 20% polyacrylamide gels (with 7 M urea to create denaturing conditions), which were autoradiographed.

2.7. *PS-A* and *PS-dC* stability in cellular extracts

An assay mixture (5 μl) containing [^{32}P]-5′-labeled dimer (11 μM), buffer H and the cytosolic fraction of A549 cell lysate (15 μg total protein

content) was incubated at room temperature for 0.5 h or 2 h. The reactions were terminated by adding deionized formamide (5 μl) containing 0.1% bromophenol blue, and the samples were analyzed by electrophoresis in a 20% polyacrylamide gel under denaturing conditions. The resulting gels were autoradiographed and analyzed.

2.8. Complex formation

Phosphorylated [^{32}P] substrates (0.06 nmol, 11 μM) were mixed with rabbit Hint1 enzyme (0.475 nmol) or cellular extract (15 μg of total protein) in buffer H for the Hint1 enzyme (the total volume of the mixture was 5 μl), cooled on ice and crosslinked at 312 nm or 254 nm (120 mJ over 2 × 10 min at 5 min intervals). Next, the samples were loaded onto 6% polyacrylamide native gels in 0.5 TBE buffer (gel retardation assay). The resulting gels were subjected to autoradiography and analyzed. The crosslinking efficiency was measured for **PS-A1a**-S_PS_P using denaturing 20% PAGE (quantification was performed on a Molecular Dynamics PhosphorImager).

In a competitive photocrosslinking reaction, the **T-PO-A** competitor (0.06, 0.12, 0.24 or 0.42 nmol) was added to a reaction (0.06 nmol **PS-A3**, 0.228 nmol rabbitHint1 and buffer H in a total volume of 5 μl), and then the mixture was irradiated at 312 nm as described above. The samples were loaded onto a 20% polyacrylamide gel with 7 M urea (denaturing conditions) in a TBE buffer, and electrophoresis was conducted. The resulting gels were subjected to autoradiography and analyzed.

2.9. Modeling

Ligand docking studies were initially performed using an Autodock Vina suite [31]. The structure of human Hint1 protein (PDB ID: 3TW2) [32] was used as a protein model. Ligand molecules were built by using the JLigand program from the CCP4 suite [33]. Of the calculated ligand molecule positions, those located in the binding pocket were chosen. For the best-fit molecules, some manual fitting (employing knowledge of the AMP binding mode) was performed. The figures were created with PyMOL (DeLano Scientific, Palo Alto, California, USA).

2.10. HINT1 gene silencing in A549 and HeLa cells by siRNAs

RNA oligonucleotides were synthesized and purified using a previously described method [34]. The sequences of synthesized RNA molecules and their complements are listed in Table 2. The purities and identities were assessed by polyacrylamide gel electrophoresis and MALDI-TOF mass spectrometry. The siRNA duplexes were prepared by mixing equimolar amounts of complementary sense and antisense RNA strands (the final duplex concentration was 20 μM), heating at 95 °C for 2 min and slowly cooling down to room temperature over 3 h. The duplex formation was analyzed by electrophoresis in a 4% agarose gel.

Twenty-four hours prior to the experiment, cells were seeded into 6-well plates at a density of 500,000 cells per well. The next day, the medium was replaced with fresh RPMI 1640 medium supplemented with 10% FBS without antibiotics, and the cells were transfected with the siRNA duplexes (siRNA-H1, control siRNA) at a 100 nM concentration using the Lipofectamine 2000 transfection reagent (Invitrogen/Life Technologies). The lipofectamine:siRNA ratio was 1 μl:1 μg. The transfection mixture contained Lipofectamine 2000 complexed with siRNA in OPTI MEM medium (Gibco/Life Technologies). The cells were incubated with the transfection reagent overnight, and the medium was replaced with fresh culture medium containing antibiotics. RNAi efficiency was evaluated 48 h after transfection by Western blot analysis. Nonspecific siRNA was used as a control [35].

2.11. Purification of adenosine 5′-O-phosphorothioate (AMPS)

To remove lithium ions, methanol, and acetonitrile from commercially available AMPS (Sigma-Aldrich), the lithium cation was exchanged for sodium and the resulting solution was vacuum-dried. A 0.5 M AMPS solution was supplemented with 1 M NaF (Sigma-Aldrich), yielding a 1-to-1 Li^+ to F^- stoichiometry. The precipitating salt, LiF (lithium fluoride has a low solubility (0.0501 M [36]), was removed by centrifugation at 13,000 *g* for 10 min at 4 °C. The supernatant was vacuum-dried at room temperature. The AMPS purity was determined by HPLC, and a single AMPS peak was detected. In this procedure, 95% of the lithium present in the original AMPS sample was exchanged with sodium cations.

2.12. Desulfuration assay

The AMPS samples (200 μM in buffer H) and 10 μg of total protein from the cytosolic fractions of the A549 or Hela cell lysates (total volumes of 10 μl each) were incubated for 120 min at 30 °C. The reaction mixtures were quenched by cooling on ice, and they were analyzed using an HPLC on a BDS Hypersil C18 column (5 μm, 250 × 4.6 mm) with a 0–17% acetonitrile gradient in 0.1 M triethylammonium bicarbonate (pH 7.4) for 15 min at a flow rate of 1 ml/min. Desulfuration levels were measured by comparing the amounts of remaining AMPS and resulting AMP, and the AMP formation percentage was calculated. Each experimental point represents the mean ± SE from measurements performed in triplicate. Statistical analysis was performed by *t*-test, and data demonstrating $p < 0.05$ were considered statistically significant.

3. Results and discussion

3.1. Design of nucleoside phosphorothioates suitable for photocrosslinking experiments that were not hydrolyzed by Hint1

Numerous Hint1 crystal structures have been reported, either in the *apo* state [37] or in complexes with different ligands [38,39], and a complex containing adenosine has been resolved at a 1.1 Å resolution [40]. However, none of the complexes contained a phosphorothioate (PS) nucleoside. To identify direct interactions between Hint1 and (d)NMPS, we synthesized phosphorothioate derivatives of AMP and dCMP (**PS-A** and **PS-dC**, respectively, Fig. 2) that were not hydrolyzed by Hint1 but did possess a moiety suitable for photocrosslinking experiments. **PS-A** and **PS-dC** are phosphorothioate nucleotide analogs that resemble dinucleoside tetraphosphates (Np_4N), in which two central phosphate groups were replaced by a trimethylene linker. The rational bases of choosing these analogs are presented in the supplementary file.

Given the chirality of both phosphorus atoms (#1 and #2), **PS-A** and **PS-dC** (which were prepared by non-stereocontrolled methods) may exist as mixtures of four P-diastereoisomers (S_PS_P, R_PS_P, S_PR_P and R_PR_P), which can in principle be chromatographically separated into pure diastereomers. The idea of determining the configuration at the P-atoms of each **PS-A** fraction is presented in the supplementary file. The results of the enzymatic tests on the **PS-A** P-diastereomers and the assigned configurations are presented in Table 1. The absolute configurations are used in the text.

3.2. Non-hydrolyzable probe complexes with recombinant rHint1 protein

PS-A and **PS-dC** were intended to form complexes with the enzyme without subsequent hydrolysis. To evaluate their function, both compounds ([^{32}P]-5′-end-labeled) were assayed as substrates for Hint1 under conditions that were highly favorable for their hydrolysis (a 1:1 enzyme:substrate molar ratio and incubation for 5 and 20 h at 37 °C). An electrophoretic analysis of the reacting mixtures and autoradiography of the resulting gels revealed no hydrolysis products shorter than substrate dimers (resulting from P–O or P–C bond cleavage, data not

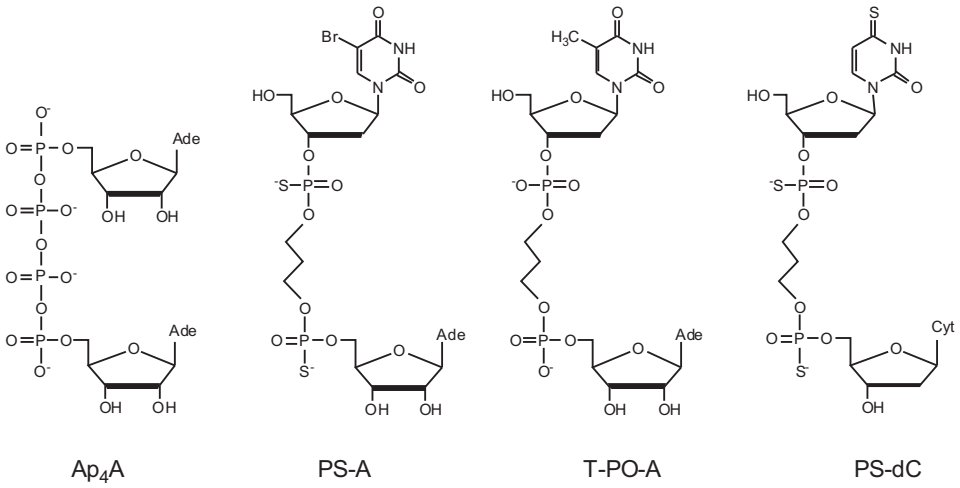

Fig. 2. Ap_4A and analogs of AMPS and dCMPS that were synthesized for photocrosslinking reactions.

shown). To prevent any enzymatic activity of Hint1 (even below 5%), all further photocrosslinking experiments were performed on ice.

Based on the known structure of Hint1, we presumed that for the **PS-A** and **PS-dC** complexes with Hint1, the photoreactive residues (5Br-dU or 4S-dU) would locate nearby Trp123, *i.e.*, in a position suitable for photocrosslinking. To form the complexes, [^{32}P]-5′-labeled **PS-A** substrates (S_PS_P and S_PR_P, 0.06 nmol, 11 μM) were mixed with the recombinant enzyme at a 1:8 molar ratio, and after incubation (5 min), the samples were irradiated with either 254 or 312 nm UV light (120 mJ, for details see the Materials and methods section) to produce stable covalent complexes. After 10 or 20 min of irradiation, the samples were loaded onto a 6% native polyacrylamide gel (gel retardation assay), and the retardation of the labeled nucleo-protein complexes (Fig. 3, arrow a) in comparison to the unbound labeled probes (Fig. 3, arrow b) was assessed after autoradiography. During this kind of analysis the unbound protein was not visible. In terms of efficiency, the photocrosslinking performed at 312 nm was better than that at 254 nm (Fig. 3) because significantly larger amounts (2–3-fold, by densitometry) of covalent products were observed at both 10 min and 20 min reaction time points. As expected, longer exposures to UV light produced greater amounts of nucleo-protein complexes. As controls, 5′-[^{32}P]-**PS-A1b** (control 1) and 5′-[^{32}P]-**PS-A1a** (control 2) alone, without the presence of the enzyme were loaded onto the gel.

In the following experiments performed under optimized conditions (irradiation at 312 nm for 2 × 10 min), all **PS-A** and **PS-dC** diastereomers were found to form complexes with recombinant rabbit Hint1 (rHint1) but at different abundances (Fig. 4, arrow a). Our previous studies with AMPS and dCMPS (P-achiral substrates) indicated that AMPS (a purine ribonucleotide) is a better substrate for rHint1 than dCMPS, which is a pyrimidine 2′-deoxyribonucleoside [4]. The results presented in Fig. 4 (panels a and b) show that the efficiency of complexing/photocrosslinking did not follow a simple "substrate" correlation because the complexes of stereodefined (R_PS_P)-**PS-A3** (panel b) and **PS-dC2** (panel a) were more abundant than those of other **PS-A** isomers and of **PS-dC1**. This finding suggests that the stereochemistry of both phosphorothioate centers influences the complexing/photocrosslinking process. We found that among the four **PS-A** isomers that interacted with rHint1, the diastereomer (R_PS_P)-**PS-A3** (containing phosphorus atom #2 of the S_P configuration) furnished the prevalent crosslinked product (taken as 100%). The next highest efficiency (by densitometry) was 61% for (S_PS_P)-**PS-A1a**, and much lower values were obtained for both isomers that had phosphorus atom #2 of R_P absolute configuration, *i.e.*, 28% for (R_PR_P)-**PS-A2** and 19% for (S_PR_P)-**PS-A1b** (Fig. 4c). These results are consistent with the data published on the substrate

Table 1
Absolute configurations of the P-atoms in P-diastereomers of **PS-A**, as listed in the 5′ → 3′ direction and determined by enzymatic digestion with svPDE and, independently, with nP1. "+" and "–" signs indicate hydrolysis or lack of hydrolysis, respectively.

Substrate	svPDE (#2-P)	nP1 (#1-P)	Absolute configurations
PS-A1a	+	+	S_PS_P
PS-A1b	–	+	S_PR_P
PS-A2	–	–	R_PR_P
PS-A3	+	–	R_PS_P

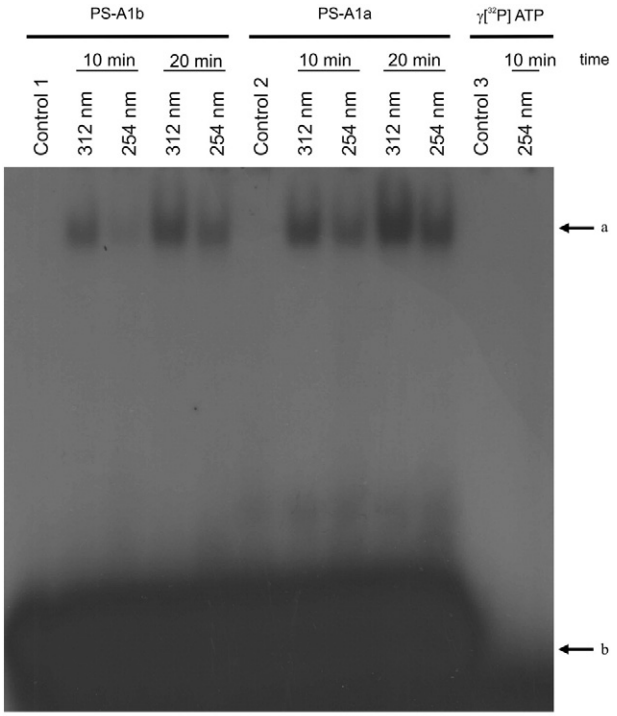

a – 5'-[^{32}P]- labeled nucleo-protein complex (with Hint)

b – unbound 5'-[^{32}P]- labeled dinucleotide substrate

Fig. 3. The autoradiogram from the gel retardation assay (non-denaturing conditions) of the complexes made by 5′-[^{32}P]-labeled two **PS-A** diastereomers (**1a** and **1b**) and recombinant rabbit Hint1 (non-labeled), as fixed by photocrosslinking at 254 nm and 312 nm, over different reaction times (10 min and 20 min). As controls, 5′-[^{32}P]-**PS-A1b** (control 1) and 5′-[^{32}P]-**PS-A1a** (control 2), without the enzyme present, were loaded. Major products of the nucleo-protein interactions are marked by arrows as 'a'.

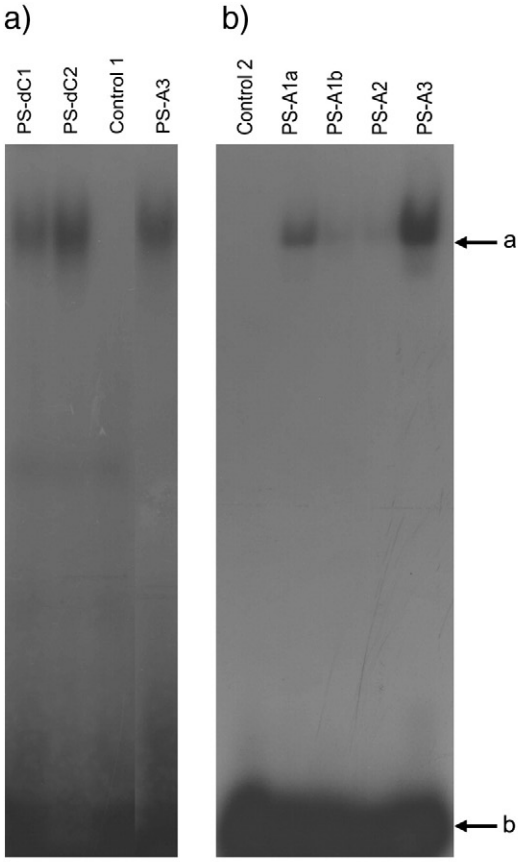

a – 5'-[^{32}P]- labeled nucleo-protein complex (with Hint)

b – unbound 5'-[^{32}P]- labeled dinucleotide substrate

c)

dimer	**PS-A1a** S_PS_P	**PS-A1b** S_PR_P	**PS-A2** R_PR_P	**PS-A3** R_PS_P
rHint1	61% ± 12	19% ± 6	28% ± 10	100%

*the amount of complex was normalized to the **PS-A3**-R_PS_P isomer, which was set as 100%.

Fig. 4. The autoradiogram from the gel retardation assay (non-denaturing conditions) of photochemically stabilized complexes comprised of recombinant rHint1 with (a) two 5′-[^{32}P]-**PS-dC** fractions and control 1–5′-[^{32}P]-**PS-dC1** without the enzyme present and (b) four 5′-[^{32}P]-**PS-A** fractions (pure P-diastereomers) and control 2–5′-[^{32}P]-**PS-A1a** without the enzyme present. Major products of the nucleo-protein interactions are marked by arrows as 'a'. (c) The percentage of a given complex formed with the participation of each **PS-A** isomer is normalized to the **PS-A3** isomer.

stereoselectivity of Hint1 towards AMPS-*N*-Trp, in which the R_P isomer was preferentially hydrolyzed [41]. By applying the Cahn–Ingold–Prelog rules, it can be concluded that the spatial orientations of the 5′-oxygen, non-bridging oxygen and sulfur atoms in the **PS-A** molecules with an S_P configuration at phosphorus #2 are analogous to those of (R_P)-AMPS-*N*-Trp.

To a certain extent, the configuration of phosphorus atom #1 also influenced the photocrosslinking results because the R_P diastereomers interacted more efficiently than in the S_P configuration (**A2** was 28% *versus* **A1b** at 19% and **A3** at 100% *versus* **A1a** at 61%). Additionally, the (R_PS_P)-**PS-A3** probe was the last eluted P-diastereomer of **PS-A** during the DMT-ON HPLC purification step. Because **PS-dC2** is also a slow eluted mixture of the 5′-*O*-DMT-tagged P-diastereomers, it can be assumed that the probes in the **PS-dC2** fraction have phosphorus atoms #1 of the R_P configuration and differ for the configuration of phosphorus #2. This assumption is supported by the results of numerous HPLC separations of 5′-*O*-DMT-tagged phosphorothioate dinucleotides (or longer oligomers) in which the separation was always strictly correlated with the absolute configuration of the P-atom closest to the 5′-ends, and the P-diastereomers of the R_P configuration had longer retention times than their S_P counterparts [42].

Moreover, a free dinucleotide probe either does not undergo the photocrosslinking process (does not crosslink to itself), or this process is of low abundance (data not shown), which is in agreement with the literature showing that irradiation at 308 nm of a free 5Br-U nucleotide in water does not lead to inactivation (that is, dimer formation) because the reaction between the nucleoside and protein results from the excitation of the aromatic amino acid residue and its anion rather than from the excitation of 5Br-U [43].

Another indication of site-specific interactions between Hint1 and the **PS-A** probe was obtained from an experiment in which the competitor (**T-PO-A**) was added to a photocrosslinking mixture that already contained **PS-A3** (0.06 nmol) and rHint (at molar ratio 1: 4) before irradiation at 312 nm. The competitor was a non-modified **PS-A** analog containing the phosphates instead of the phosphorothioates and the thymidine residue instead of 5Br-dU (Fig. 2). We expected that **T-PO-A** would compete with **PS-A3** for the same enzyme domain, and after irradiation, the total amount of **PS-A3**/rHint1 nucleo-protein complex would be lower than it was without the competitor. Indeed, we found increasing amounts of **T-PO-A** (from 0.06 to 0.42 nmol, the molar ratios of **PS-A3**:**T-PO-A**:rHint1 were as follows: 1:1:4, 1:2:4, 1:4:4 and 1:7:4), which decreased the level of **PS-A3**/rHint1 complex formation (Fig. 5). This result indicates that both compounds compete for the same site (most likely the catalytic center) on the enzyme, and furthermore, **PS-A3** does not bind randomly to Hint1. In the independent experiment, the potential formation of a covalent bond between **T-PO-A** and rHint1 after 312 nm UV irradiation was evaluated. We observed the formation of nucleo-protein below 1% when compared with **PS-A1a** (data not shown).

Therefore, these results confirmed our assumptions that the interactions of diastereomeric substrates with the enzyme under study are specific and stereo-dependent.

3.3. Modeling

Based on our results and the crystal structure of Hint1 in complex with AMP [32], we wanted to propose some possible interactions between **PS-A** and Hint1. The L1, L3 and L6 loop regions of the protein (which were involved in building the binding groove) were previously shown to be flexible (see Fig. 6b). To support our assumption that the **PS-A3** ligand can fit into the catalytic center, the docking process was performed by employing knowledge of the binding mode of AMP. The **PS-A3** molecule was placed in the "active" orientation, and thus the adenosine residue interacts with the hydrophobic purine-binding pocket and the sugar-binding pocket. Thus, Asp43 makes hydrogen bonds with the O2′ and/or O3′ oxygen atoms of the ribose ring, and oxygen atoms of the 5′-*O*-phosphate group interact with His112 and His114 as reported previously [4,39]. The flexible trimethylene linker placed the 5Br-dU outside the protein. We found a possible arrangement in which stacking interactions between Trp123 and 5Br-dU residues becomes feasible (Fig. 6a). In addition, the distance between the C-5 atom of uracil and the C-2 atom of Trp123 is appropriate for the formation of a covalent bond. The docking results are presented in Fig. 6. To better understand the accessible space, the protein surface was visualized for the Hint1 dimer, and the ligand in the binding pocket is shown with sticks (Fig. 6b).

Fig. 5. The autoradiogram from PAGE analysis (denaturing conditions) of the competitive photocrosslinking reaction of 5′-[^{32}P]-labeled **PS-A3** (0.06 nmol) and rHint1 (0.23 nmol) in the presence of the **T-PO-A** competitor (non-labeled). The amounts of **T-PO-A** added are from 0.06 to 0.42 nmol (as noted at the top of each channel), and the molar ratios of **PS-A3**:**T-PO-A**:rHint1 are as follows: 1:1:4, 1:2:4, 1:4:4 and 1:7:4 . The products of the nucleo-protein interactions are marked by arrows as 'a'.

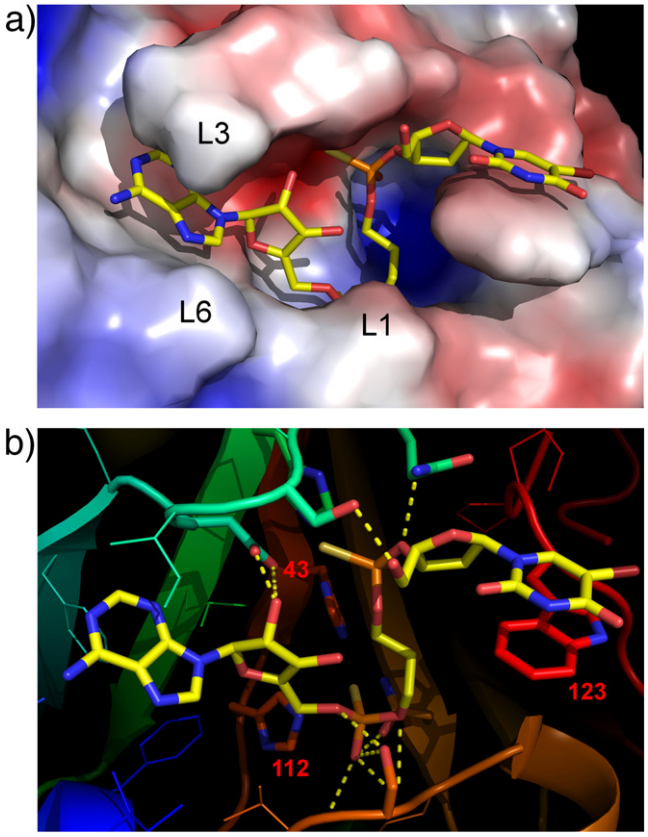

Fig. 6. The docking of **PS-A3** at the catalytic center of Hint1 (created with PyMOL, DeLano Scientific, Palo Alto, California, USA). The ligand molecule is shown with a stick representation, and the sulfur atoms are indicated in dark yellow. (a) The protein chains are shown with cartoon representations. Selected protein residues involved into ligand binding are shown as sticks. The stacking interactions between the Trp123 and 5Br-dU residues are visible. (b) The protein dimer is shown with a calculated electrostatic surface (blue is positive and red is negative). The **PS-A3** molecule fills the binding pocket. L1, L3 and L6 are the flexible loop regions enclosing the binding cleft.

As mentioned, the stereochemistry of both phosphorothioate linkages in **PS-A** plays a role in complex formation. It is worth noting that the modeling data indicate that the spatial orientation of both sulfur atoms in (R_PS_P)-**PS-A3** offers the fewest disturbing contacts with the enzyme, and in the photocrosslinking studies, this particular diastereomer forms the complex most efficiently. Thus, the experimental and modeling data are convergent.

3.4. Formation of complexes with the proteins present in the cytosolic fraction of A549 cellular extracts

To select an appropriate cell line, Hint1 levels in cellular extracts from A549, HeLa, HL60, HUVEC, Neuro2A and SY5Y cells were assessed by Western blot analysis. The A549 cell line was chosen for further studies based on having the highest protein levels (data not shown). These cells exhibited Fhit negative status (Fhit$^-$) [44]. This finding is important because if they were Fhit$^+$, unwanted competitive interactions with the probes might occur because the Fhit protein belongs to the HIT superfamily [1] and is able to desulfurate AMPS (albeit not very efficiently) [4,41]. Although HeLa cells were also Fhit$^-$ and demonstrated only slightly lower amounts of Hint1 than A549 cells, they were rejected because their high phosphatase activity could make the analysis of [^{32}P]-5′-labeled substrates very difficult or impossible. According to the literature, Hint1 is a cytosolic protein [1], and for our additional experiments, we used the cytosolic fraction of an A549 cellular extract (Fig. S2, supplementary).

We then checked the stability of **PS-A** and **PS-dC** ([^{32}P]-labeled at the 5′-ends) under the conditions used for complex formation. Both compounds were mixed with the cytosolic fraction of A549 cells (cytA549). Following incubation (0.5 or 2 h, room temperature), the dephosphorylation levels were not higher than 30% or 60%, respectively, when compared with the reaction with an added phosphatase inhibitor (Fig. S3, supplementary). No degradation was observed after 2 h of incubation at 4 °C (data not shown).

In the photocrosslinking experiments, the 5′-[^{32}P]-**PS-A** and 5′-[^{32}P]-**PS-dC** fractions were incubated with cytA549 to form the nucleoprotein complexes, which were irradiated after 5 min with light at 312 nm (2 × 10 min, ice-cooled samples). Both compounds formed few complexes with the proteins present in the samples. One of these proteins was identified as Hint1 based on the similarity of the electrophoretic mobility of the complex to that of the reference complex formed with recombinant Hint1 (Fig. 7). It should be pointed out that stereodifferentiation was observed during the formation of complexes between cellular Hint1 and different P-diastereomers of 5′-[^{32}P]-**PS-A**, and this followed the stereodifferentiation described for complexation with the recombinant Hint1 protein. The 5′-[^{32}P]-**PS-dC** derivatives formed the complexes less efficiently than the 5′-[^{32}P]-**PS-A** analogs. These results suggest that nucleoside 5′-*O*-

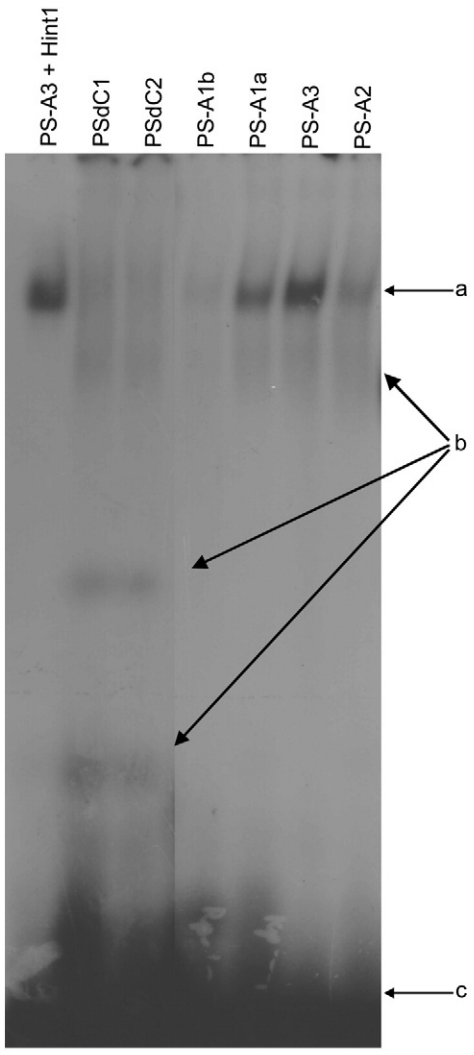

Fig. 7. The autoradiogram from the gel retardation assay (non-denaturing conditions) of the photocrosslinked complexes formed by the fractions of labeled 5′-[^{32}P]-**PS-A** and 5′-[^{32}P]-**PS-dC** with non-labeled Hint1 which was present in the cytosolic fraction of the A549 cell lysate. As a mobility control, the photocrosslinked complex of 5′-[^{32}P]-**PS-A3** with non-labeled recombinant Hint1 was used (line 1). Major products of the nucleo-protein interactions are marked by arrows as 'a'.

phosphorothioates may be recognized and perhaps hydrolyzed by Hint1 inside the cells.

3.5. Generation of siRNA directed towards HINT1 mRNA

We generated siRNAs targeted towards HINT1 mRNA[1] and evaluated their ability to down-regulate HINT1 gene expression in A549 and Hela cells. Two pairs of oligomers were synthesized, specifically the HINT1 targeted sense strand (H1S), the HINT1 targeted antisense strand (H1AS), the control sense strand (CS) and the control antisense strand (CAS) (Table 2). The oligomer molecular masses were confirmed by MALDI-TOF mass spectrometry, and their ability to form siRNA duplexes was observed by electrophoresis in a 4% agarose gel (data not shown). Western blot analysis of the cytosolic fractions from cells treated with the siRNA H1 indicated (Fig. 8) that 48 h after transfection, Hint1 protein levels had decreased by 65% and 46% in A549 and HeLa cells, respectively, when compared with the cells transfected with the non-specific siRNA duplex control.

[1] Ozga M. (2010) Ph.D. thesis (in Polish), CMMS PAS.

Table 2
siRNA sequences of the sense (S) and antisense strands (AS) used in the desulfuration studies.

siRNA	Strand	Sequences
H1	S	5′-CCUCAAGCACCAACACAUUTT-3′
	AS	3′-TTGGAGUUCGUGGUUGUGUAA-5′
Control	S	5′-AAUCAGAUUGAACCUUCAUTT-3′
	AS	3′-TTUUAGUCUAACUUGGAAGUA-5′

3.6. Desulfuration of AMPS using cellular lysates

To show that the desulfuration process can occur with participation of the enzyme which is present in the cell together with other proteins and at low cellular concentration, protein extracts of A549 and HeLa cells were used for reactions with AMPS. AMPS was added (for a final concentration of 200 μM) to the isolated cytosolic fractions, and the mixtures were incubated for 2 h. The reaction progress was controlled *via* the HPLC method. For both cell lines, the desulfuration of AMPS occurred according to the following equation:

$$\text{AMPS} \xrightarrow{\text{cytA549orcytHeLa}} \text{AMP} + H_2S\uparrow$$

We assumed that Hint1 participates in this process and to verify this hypothesis, HINT1 gene expression was down-regulated using the siRNA methodology described above (HINT1-targeted siRNA duplexes). The reactions with AMPS were conducted as described previously; however, they employed the cytosolic fractions of both cell lines as isolated after an siRNA H1 application. The cytosolic fractions of lysates from cells that were transfected with a non-specific siRNA duplex were used as controls. The samples were analyzed by HPLC, and desulfuration levels were measured by comparing the amounts of remaining AMPS and resulting AMP. The AMP contents of A549 and Hela cells treated with the HINT1-targeted siRNA H1 duplex were lower (2 and 2.7 times, for A549 and HeLa, respectively) when compared with cells treated with control duplex siRNA (Fig. 9). In control experiments, no spontaneous desulfuration of AMPS was observed even after 20 h of incubation under analogous reaction conditions (thermally deactivated cytosolic fractions). Adding phosphatase inhibitors (NaF and imidazole, 2 mM each) did not change the composition of the reaction products. Although the desulfuration experiments were conducted using enzymatically active

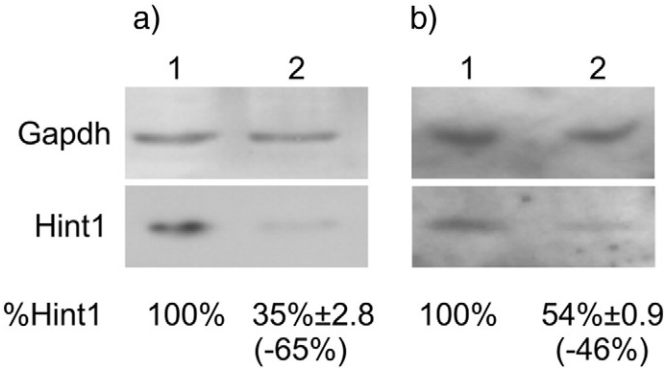

Fig. 8. Western blot analysis of the Hint1 protein levels in the cytosolic fractions of (a) A549 and (b) HeLa cells transfected with control non-specific siRNA (lanes 1) and with siRNA H1 (lanes 2).

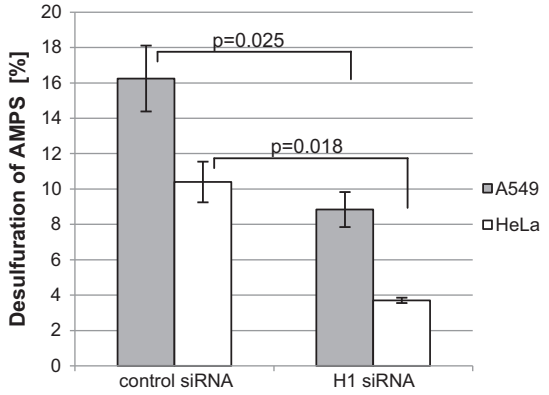

Fig. 9. Comparison of the percentage of the AMPS → AMP conversion in the reactions of the cytA549 and cytHela with and without silenced Hint1 expression ($P < 0.05$). Both cells line were treated with HINT1-targeted and control siRNA duplexes and then cytosolic fractions were isolated and used. The reaction progress was analyzed *via* the HPLC method and desulfuration levels were measured by calculation of the amounts of remaining AMPS and resulting AMP.

cellular lysates of different cell lines, we do believe that the results strongly support our hypothesis that intracellular Hint1 is involved in the desulfuration process of model adenosine-5′-*O*-monophosphorothioate *in vivo*. Additionally, taking into account our previous report [4], which showed that the Hint1 enzyme was able to hydrolyze monophosphorothioate nucleosides of both the ribo- and 2′-deoxyribonucleoside series, we postulate that other (d)NMPS can also be intracellularly desulfurated by the Hint1 protein.

4. Conclusions

We used various methods and non-hydrolyzable derivatives of 5′-*O*-adenosine and deoxycytidine phosphorothioates (AMPS and dCMPS) to demonstrate the direct interactions between (d)NMPS and the Hint1 protein in the enzyme active site. We found that after photocrosslinking the non-hydrolyzable derivatives formed stable covalent complexes with recombinant rHint1. Moreover, the interactions of the diastereomeric substrates with the enzyme appeared to be stereo-dependent because different diastereomers formed the complexes with different efficiency. The competitive photocrosslinking reaction of pure Hint1 with the selected non-hydrolyzable diastereoisomer of **PS-A3** in the presence of the **T-PO-A** competitor confirmed the site-specific interactions between the enzyme under study and the substrate analog. In summary, it was demonstrated that the interactions of diastereomeric substrates with Hint1 are specific and stereo-dependent.

Computer modeling experiments in which the **PS-A3** ligand was docked at the binding cleft confirmed that direct interactions between Hint1 and the studied ligands are geometrically possible. Next, AMPS and dCMPS derivatives were used as a bait to trap Hint1 in the mixture of proteins present in the cytosolic fraction of an A549 cellular lysate. After fixing by photocrosslinking and analyzing samples by electrophoresis, we found that these non-hydrolyzable substrate analogs were able to form complexes with cellular Hint1, and the stereochemistries of both phosphorothioate centers influence the complexing/photocrosslinking process, as was found for the recombinant protein. Therefore, we conclude that under cellular conditions the interactions between Hint1 and nucleosides phosphorothioate are possible which indicates the possibility of occurrence of such effects *in vivo*.

The most significant experiment provided evidence for the participation of cellular Hint1 in the enzymatic conversion of AMPS to AMP. In the reactions the cellular lysates were used, which contained the enzymatically active mixtures of proteins (including Hint1). Using RNAi technology, we demonstrated decreased levels of substrate desulfuration for the reactions in which the cell lysate with reduced Hint1 expression was used compared to the reaction employing the cell lysate with the normal Hint1 level.

Our previous results [4] revealed the hydrolytic activity of Hint1 towards different nucleoside 5′-*O*-phosphorothioates. We also demonstrated that the mechanism of (d)NMPS desulfuration is similar to P–N bond cleavage in phosphoramidate substrates. Taking all of these observations together (from previous and present studies), we conclude that the intracellular Hint1 enzyme could be responsible for the desulfuration of nucleosides 5′-*O*-monophosphorothioate in cells. Because *Hint1* orthologs have been found across the spectrum from prokaryotes to eukaryotes, this protein may participate in the metabolism of phosphorothioate oligonucleotides and phosphorothioate DNA segments *in vivo*. The enzymes responsible for the *in vivo* degradation of phosphorothioate oligonucleotides to 5′-monophosphorothioate nucleotides are well known [24,25], while the next step — degradation of (d)NMPSs remains unknown. One of the subsequent steps could be the conversion of (d)NMPS to (d)NMP, which most probably occurs with participation of Hint1, so this enzyme seems to be responsible for the next step of PS-oligo metabolism. We are aware that there could also be other enzymes (*e.g.*, Hint2) that participate in the desulfuration of (d)NMPS *in vivo* and further studies are in progress.

Moreover, if the removal of (d)NMPS from the cells requires their conversion to (d)NMP *via* the mechanism producing free hydrogen sulfide, then it would be valuable to measure the amount of gas that is released during the desulfuration reaction inside cells. Biomedical research on H_2S is still in an early phase and specific H_2S donors, offering physiological doses (nontoxic for a long time) are demanded for investigation on the properties and functions of H_2S in biological systems. Inorganic sulfide salts (eg. Na_2S or NaHS) are not good donors because they provide supraphysiological, toxic concentration of H_2S in a short time. In our previous study, we demonstrated different rates of H_2S release by Hint1, depending on the NMPS used [4]. So, such a regulation of H_2S concentration in an organism could indicate a possible therapeutic value of (d)NMPSs as the precursors of H_2S *in vivo*. The new H_2S donors have already been considered as potential drugs for the treatment of cardiovascular, neurological and inflammatory diseases [45]. As a result, we believe that controlled delivery of (d)NMPSs into cells could offer a new way to change the levels of this gaseous signaling molecule and further studies are in progress.

Acknowledgments

The authors are grateful to Dr. Piotr Guga for his critical discussions.

This work was supported by the Polish Ministry of Science and Higher Education grant no NN204130137 and by The National Science Centre grant no DEC-2013-/09/B/ST5/03612 to AK.

Appendix A. Supplementary data

Supplementary data to this article can be found online at http://dx.doi.org/10.1016/j.bbagen.2014.08.016.

References

[1] C. Brenner, Hint, Fhit, and GalT: function, structure, evolution, and mechanism of three branches of the histidine triad superfamily of nucleotide hydrolases and transferases, Biochemistry 41 (2002) 9003–9014.
[2] P. Bieganowski, P.N. Garrison, S.C. Hodawadekar, G. Faye, L.D. Barnes, C. Brenner, Adenosine monophosphoramidase activity of Hint and Hnt1 supports function of Kin28, Ccl1, and Tfb3, J. Biol. Chem. 277 (2002) 10852–10860.
[3] T.F. Chou, I.B. Tikh, B.A. Horta, B. Ghosh, R.B. De Alencastro, C.R. Wagner, Engineered monomeric human histidine triad nucleotide-binding protein 1 hydrolyzes fluorogenic acyl-adenylate and lysyl-tRNA synthetase-generated lysyl-adenylate, J. Biol. Chem. 282 (2007) 15137–15147.
[4] M. Ozga, R. Dolot, M. Janicka, R. Kaczmarek, A. Krakowiak, Histidine triad nucleotide-binding protein 1 (HINT-1) phosphoramidase transforms nucleoside

5′-*O*-phosphorothioates to nucleoside 5′-*O*-phosphates, J. Biol. Chem. 285 (2010) 40809–40818.
[5] A. Guranowski, A.M. Wojdyła, J. Zimny, A. Wypijewska, J. Kowalska, M. Łukaszewicz, J. Jemielity, E. Darzynkiewicz, A. Jagiełło, P. Bieganowski, Recognition of different nucleotidyl-derivatives as substrates of reactions catalyzed by various HIT-proteins, New J. Chem. 34 (2010) 888–893.
[6] T.F. Chou, J. Baraniak, R. Kaczmarek, X. Zhou, J. Cheng, B. Ghosh, C.R. Wagner, Phosphoramidate pronucleotides: a comparison of the phosphoramidase substrate specificity of human and *Escherichia coli* histidine triad nucleotide binding proteins, Mol. Pharm. 4 (2007) 208–217.
[7] J. Weiske, O. Huber, The histidine triad protein Hint1 triggers apoptosis independent of its enzymatic activity, J. Biol. Chem. 281 (2006) 27356–27366.
[8] J. Weiske, O. Huber, The histidine triad protein Hint1 interacts with Pontin and Reptin and inhibits TCF-β-catenin-mediated transcription, J. Cell Sci. 118 (2005) 3117–3129.
[9] M. Rodríguez-Muñoz, J. Garzón, Nitric oxide and zinc-mediated protein assemblies involved in mu opioid receptor signaling, Mol. Neurobiol. 48 (2013) 769–782.
[10] N. Korsisaari, T.P. Makela, Interactions of Cdk7 and Kin28 with Hint/PKCI-1 and Hnt1 histidine triad proteins, J. Biol. Chem. 275 (2000) 34837–34840.
[11] E. Razin, Z.C. Zhang, H. Nechushtan, S. Frenkel, Y.N. Lee, R. Arudchandran, J. Rivera, Suppression of microphthalmia transcriptional activity by its association with protein kinase C-interacting protein 1 in mast cells, J. Biol. Chem. 274 (1999) 34272–34276.
[12] Y.N. Lee, H. Nechushtan, N. Figov, E. Razin, The function of lysyl-tRNA synthetase and Ap4A as signaling regulators of MITF activity in FcεRI-activated mast cells, Immunity 20 (2004) 145–151.
[13] Y.N. Lee, E. Razin, Nonconventional involvement of LysRS in the molecular mechanism of USF2 transcriptional activity in FcεRI-activated mast cells, Mol. Cell. Biol. 25 (2005) 8904–8912.
[14] N. Yannay-Cohen, I. Carmi-Levy, G. Kay, C.M. Yang, J.M. Han, D.M. Kemeny, S. Kim, H. Nechushtan, E. Razin, LysRS serves as a key signaling molecule in the immune response by regulating gene expression, Mol. Cell 34 (2009) 603–611.
[15] T.-F. Chou, C.R. Wagner, Lysyl-tRNA synthetase-generated lysyl-adenylate is a substrate for histidine triad nucleotide binding proteins, J. Biol. Chem. 282 (2007) 4719–4727.
[16] T.F. Chou, P. Bieganowski, K. Shilinski, J. Cheng, C. Brenner, C.R. Wagner, ^{31}P NMR and genetic analysis establish hinT as the only *Escherichia coli* purine nucleoside phosphoramidase and as essential for growth under high salt conditions, J. Biol. Chem. 280 (2005) 15356–15361.
[17] S. Bardaweel, B. Ghosh, T.F. Chou, M.J. Sadowsky, C.R. Wagner, *E. coli* histidine triad nucleotide binding protein 1 (ecHinT) is a catalytic regulator of D-alanine dehydrogenase (DadA) activity in vivo, PLoS One 6 (2011) e20897.
[18] M. Zimon, J. Baets, L. Almeida-Souza, E. De Vriendt, J. Nikodinovic, Y. Parman, E. Battaloglu, Z. Matur, V. Guergueltcheva, I. Tournev, M. Auer-Grumbach, P. De Rijk, B.-S. Petersen, T. Muller, E. Fransen, P. Van Damme, W.N. Loscher, N. Barisic, Z. Mitrovic, S.C. Previtali, H. Topaloglu, G. Bernert, A. Beleza-Meireles, S. Todorovic, D. Savic-Pavicevic, B. Ishpekova, S. Lechner, K. Peeters, T. Ooms, A.F. Hahn, S. Zuchner, V. Timmerman, P. Van Dijck, V.M. Rasic, A.R. Janecke, P. De Jonghe, A. Jordanova, Loss-of-function mutations in HINT1 cause axonal neuropathy with neuromyotonia, Nat. Genet. 44 (2012) 1080–1083.
[19] G. Yang, L. Wu, B. Jiang, W. Yang, J. Qi, K. Cao, Q. Meng, A.K. Mustafa, W. Mu, S. Zhang, S.H. Snyder, R. Wang, H_2S as a physiologic vasorelaxant: hypertension in mice with deletion of cystathionine gamma-lyase, Science 322 (2008) 587–590.
[20] R. Wang, Toxic gas, lifesaver, Sci. Am. 302 (2010) 66–71.
[21] J.R. Koenitzer, T.S. Isbell, H.D. Patel, G.A. Benavides, D.A. Dickinson, R.P. Patel, V.M. Darley-Usmar, J.R. Lancaster Jr., J.E. Doeller, D.W. Kraus, Hydrogen sulfide mediates vasoactivity in an O_2-dependent manner, Am. J. Physiol. Heart Circ. Physiol. 292 (2007) H1953–H1960.
[22] L. Wang, S. Chen, T. Xu, K. Taghizadeh, J.S. Wishnok, X. Zhou, D. You, Z. Deng, P.C. Dedon, Phosphorothioation of DNA in bacteria by dnd genes, Nat. Chem. Biol. 3 (2007) 709–710.
[23] N. Dias, C.A. Stein, Antisense oligonucleotides: basic concepts and mechanisms, Mol. Cancer Ther. 1 (2002) 347–355.
[24] J. Temsamani, A. Roskey, C. Chaix, S. Agrawal, In vivo metabolic profile of a phosphorothioate oligodeoxyribonucleotide, Antisense Nucleic Acid Drug Dev. 7 (1997) 159–165.
[25] M. Koziolkiewicz, M. Wojcik, A. Kobylanska, B. Karwowski, B. Rebowska, P. Guga, W. J. Stec, Stability of stereoregular oligo(nucleoside phosphorothioate)s in human plasma. Diastereoselectivity of plasma 3′-exonuclease, Antisense Nucleic Acid Drug Dev. 7 (1997) 43–48.
[26] S. Agrawal, Q. Zhao, Antisense therapeutics, Curr. Opin. Chem. Biol. 2 (1998) 519–528.
[27] M. Koziolkiewicz, E. Gendaszewska, M. Maszewska, C.A. Stein, W.J. Stec, The mononucleotide-dependent, nonantisense mechanism of action of phosphodiester and phosphorothioate oligonucleotides depends upon the activity of an ecto-5′-nucleotidase, Blood 98 (2001) 995–1002.
[28] K.M. Meisenheimer, T.H. Koch, Photocross-linking of nucleic acids to associated proteins, Crit. Rev. Biochem. Mol. Biol. 32 (1997) 101–140.
[29] W.J. Stec, B. Uznanski, A. Wilk, B.L. Hirschbein, K.L. Fearon, B.J. Bergot, Bis(*O*, *O*-diisopropoxy phosphinothioyl) disulfide — a highly efficient sulfurizing reagent for cost-effective synthesis of oligo(nucleoside phosphorothioate)s, Tetrahedron Lett. 34 (1993) 5317–5320.
[30] S. Ghosh, J.M. Lowenstein, A multifunctional vector system for heterologous expression of proteins in *Escherichia coli*. Expression of native and hexahistidyl fusion proteins, rapid purification of the fusion proteins, and removal of fusion peptide by Kex2 protease, Gene 176 (1996) 249–255.
[31] O. Trott, A.J. Olson, AutoDock Vina: improving the speed and accuracy of docking with a new scoring function, efficient optimization, and multithreading, J. Comp. Chem. 31 (2010) 455–461.
[32] R. Dolot, M. Ozga, A. Wlodarczyk, A. Krakowiak, B. Nawrot, A new form of human histidine triad nucleotide-binding protein 1 (hHINT1) in complex with adenosine-5′-monophosphate at 1.38 Å resolution, Acta Crystallogr. F68 (2012) 883–888.
[33] M.D. Winn, C. Ballard Ch, K.D. Cowtan, E.J. Dodson, P. Emsley, P.R. Evans, R.M. Keegan, E.B. Krissinel, A.G. Leslie, A. McCoy, S.J. McNicholas, G.N. Murshudov, N.S. Pannu, E.A. Potterton, H.R. Powell, R.J. Read, A. Vagin, K.S. Wilson, Overview of the CCP4 suite and current developments, Acta Crystallogr. D Biol. Crystallogr. 67 (2011) 235–242.
[34] K. Sipa, E. Sochacka, J. Kazmierczak-Baranska, M. Maszewska, M. Janicka, G. Nowak, B. Nawrot, Effect of base modifications on structure, thermodynamic stability, and gene silencing activity of short interfering RNA, RNA 13 (2007) 1301–1316.
[35] M. Sierant, K. Kubiak, J. Kazmierczak-Baranska, M. Warashina, T. Kuwabara, B. Nawrot, Evaluation of BACE1 silencing in cellular models, Int. J. Alzheimers Dis. (2009) 257403 (Article ID, 10 pages).
[36] M. Windholz, The Merck Index, 10th ed. Merck, Rahway, NJ, 1983.
[37] C.D. Lima, M.G. Klein, B. Weinstein, W.A. Hendrickson, Three-dimensional structure of human protein kinase C interacting protein 1, a member of the HIT family of proteins, Proc. Natl. Acad. Sci. U. S. A. 93 (5357) (1996) 5362.
[38] C. Brenner, P. Garrison, J. Gilmour, D. Peisach, D. Ringe, G.A. Petsko, J.M. Lowenstein, Crystal structures of HINT demonstrate that histidine triad proteins are GalT-related nucleotide-binding proteins, Nat. Struct. Biol. 4 (1997) 231–238.
[39] A. Krakowiak, H.C. Pace, G.M. Blackburn, M. Adams, A. Mekhalfia, R. Kaczmarek, J. Baraniak, W.J. Stec, C. Brenner, Biochemical, crystallographic, and mutagenic characterization of hint, the AMP-lysine hydrolase, with novel substrates and inhibitors, J. Biol. Chem. 279 (2004) 18711–18716.
[40] R. Dolot, M. Ozga, A. Krakowiak, B. Nawrot, High-resolution X-ray structure of the rabbit histidine triad nucleotide-binding protein 1 (rHINT1)-adenosine complex at 1.10 Å resolution, Acta Crystallogr. D67 (2011) 601–607.
[41] A. Krakowiak, R. Kaczmarek, J. Baraniak, M. Wieczorek, W.J. Stec, Stereochemistry of rHint1 hydrolase assisted cleavage of P–N bond in nucleoside 5′-*O*-phosphoramidothioates, Chem. Commun. 2007 (2007) 2163–2165.
[42] M. Koziołkiewicz, B. Uznański, W.J. Stec, G. Zon, P-chiral analogues of oligodeoxyribonucleotides: synthesis, stereochemistry and enzyme studies, Chem. Scr. 26 (1986) 251–260.
[43] C.L. Norris, K.M. Meisenheimer, T.H. Koch, Mechanistic studies relevant to bromouridine enhanced nucleoprotein photocross-linking. Possible involvement of an excited tyrosine residue of the protein, Photochem. Photobiol. 65 (1997) 201–207.
[44] A. Krakowiak, R. Pecherzewska, R. Kaczmarek, A. Tomaszewska, B. Nawrot, W.J. Stec, Evaluation of influence of Ap(4)A analogues on Fhit-positive HEK293T cells; cytotoxicity and ability to induce apoptosis, Bioorg. Med. Chem. 19 (2011) 5053–5060.
[45] A. Martelli, L. Testai, M.C. Breschi, C. Blandizzi, A. Virdis, S. Taddei, V. Calderone, Hydrogensulfide: novel opportunity for drug discovery, Med. Res. Rev. 32 (2012) 1093–1130.